The Influence of Surface Potential on the Optical Switching of Spiropyran Self Assembled Monolayers

Tobias Garling[1,*], Yujin Tong[1,*], Tamim A Darwish[2], Martin Wolf[1], R Kramer Campen[1]

[1] Fritz Haber Institute of the Max Planck Society, Faradayweg 4-6, Berlin, Germany,
[2] Australian Nuclear Science and Technology Organisation (ANSTO), Locked Bag 2001, Kirrawee DC, NSW 2232, Australia
*These two authors contributed equally.

E-mail: campen@fhi-berlin.mpg.de

Abstract. Surfaces whose macroscopic properties can be switched by light are potentially useful in a wide variety of applications. One such promising application is electrochemical sensors that can be gated by optically switching the electrode *on* or *off*. One way to make such a switchable electrode is by depositing a self-assembled monolayer of bistable, optically switchable molecules onto an electrode surface. Quantitative application of any such sensor requires understanding how changes in interfacial field affect the composition of photostationary states, *i.e.* how does electrode potential affect the extent to which the electrode is *on* or *off* when irradiated, and the structure of the SAM. Here we address these questions for a SAM of a 6-nitro-substituted spiro[2H-1-benzopyran-2,2'-indoline] covalently attached through a dithiolane linker to an Au electrode immersed in a 0.1 M solution of Tetramethylammonium hexafluorophosphate in Acetonitrile using interface-specific vibrational spectroscopy. We find that in the absence of irradiation, when the SAM is dominated by the closed spiropyran form, variations in potential of 1 V have little effect on spiropyran relative stability. In contrast, under UV irradiation small changes in potential can have dramatic effects: changes in potential of 0.2 V can completely destabilize the open, merocyanine form of the SAM relative to the spiropyran and dramatically change the chromophore orientation. Quantitatively accounting for these effects is necessary to employ this, or any other optically switchable bistable chromophore, in electrochemical applications.

1. Introduction

Surfaces whose macroscopic properties can be switched using external stimuli are potentially useful in such diverse applications as membrane filters [1], molecular (opto)electronics [2, 3, 4, 5] and (bio)electrochemical sensors [6, 7, 8, 9, 10, 11]. Building such responsive surfaces is challenging. A wide variety of bistable molecules, *e.g.* azobenzenes, spiropyrans, and fulgides, are known to change such properties as conformation or dipole moment on external stimulus (*e.g.* light, temperature or pH) when dissolved in solution. Thus one path to the creation of functionalized surfaces is to immobilize and orient such molecules on surfaces and switch them in a concerted fashion

(thus converting a molecular scale response to a macroscopic effect). Using this strategy a number of studies have demonstrated electrochemical sensors that can be switched *on/off*: *i.e.* one state of the molecule allows its interaction with an analyte (that can be detected amperometrically [6] or potentiometrically [12]) while the other does not. Such a sensing concept is attractive because, in the *off* state the background signal can easily be quantified, and analyte can easily be washed off (and thus sensor reusability is high) [9]. Because it is noninvasive, produces few side products and can be applied precisely in space and time, light is an attractive external stimulus for such devices [13, 14].

Clearly if we wish to move beyond proof-of-principle, and towards optimization of such switchable electrochemical sensors, understanding how the thermodynamics and kinetics of switching changes with applied electric fields is important. Physical intuition suggests that applied fields could have large effects. For example, if the two forms of a bistable molecule have dramatically different dipoles, one might expect that in the presence of an applied field either the relative stability of the two forms, or the orientation of a particular form, may change. The notion that a change in surface potential, may lead to a change in structure of a SAM has been been previously demonstrated [15], but the manner in which surface fields influence the photostationary states of *optically* switchable SAMS was not addressed. While it is possible that applied fields degrade device performance through this mechanism, one might imagine also applying such effects for useful purposes. For example, Willner et al. have found it impossible to completely switch off an amperometric sensor with light due to the strong binding of an anti-dinitrophenyl antibody to their dinitrophenyl antigen monolayer on an Au electrode [6]. Clearly if a potential perturbation could reset such a sensor, and allow it to be fully switched off, this would be useful.

In this study we address the relationship between the stability/structure of the two forms of a 6-nitro-substituted spiro[2H-1-benzopyran-2,2′-indoline] (hereafter called 6–Nitro–BIPS) covalently attached to a gold electrode as a function of applied field. The photochromism of 6–Nitro–BIPS has been well investigated in solution [16]. Irradiation with light at UV frequencies leads to a breaking of the C–O–Bond at the spirocentre in the spiropyran(SP)–form, yielding, after a number of intermediates, the merocyanine(MC)–form (see Figure 1) on timescales, to reach the photostationary state of the ensemble, of seconds (with the precise time dependent on concentration and irradiation). In contrast to the SP–form the MC–form is zwitterionic and planar with a conjugated electronic system and thus SP→MC switching results in a large change in dipole moment (from 5 to 16 D[17]) and the appearance of a new band in the visible absorption spectrum [17, 16]. In solution the photostationary state is reached after back switching, MC→SP, under irradiation with vis–light in tens of minutes or thermally in hours [16].

Prior work investigating photoswitchable self-assembled-monolayers on surfaces has shown that minimizing chromophore/chromophore steric interaction and chromophore/solid coupling is key in the preserving the solution phase activity of bistable molecules in the surface environment [18, 19, 20, 21]. Here, following prior work by Browne and coworkers and some of us, we minimize these unwanted effects by attaching

6–Nitro–BIPS to a gold surface via a linker chain containing a dithiolane anchoring group (*i.e.* we characterise a SAM of 2-(3'3'-Dimethyl-6-nitro-3'H-spiro[chromene-2,2'-indol]-1'-yl)ethyl(1,2-dithiolane-3)pentanoate (hereafter called SP-LA) on gold (see Figure 1) [22, 23]. In addition to its switch related benefits, this chemistry has the advantage of being relatively practical: gold is relatively easy to prepare in thin films and stable in air [24], gold thiol chemistry is well described in the literature and thus stable SAMS are relatively easy to fabricate [25].

However, even in the absence of strong chromophore/Au interaction surface fields may affect the structure of the SP-LA monolayer, or the relative concentrations of MC and SP forms, in the monolayer's photostationary states. To assess such effects we require a method capable of probing the structure of conformationally flexible molecules within a nm of an electrode surface (and thus at a solid/liquid interface). There are few experimental techniques that offer such insight. Here we employ the interface-specific, non-linear optical technique vibrational sum frequency (VSF) spectroscopy as a function of applied potential [26, 27] to probe our 6–Nitro-BIPS SAM at the gold/electrolyte interface. We show that, well within a potential region of SAM stability, optical switching can be suppressed completely and reversibly as a function of applied potential.

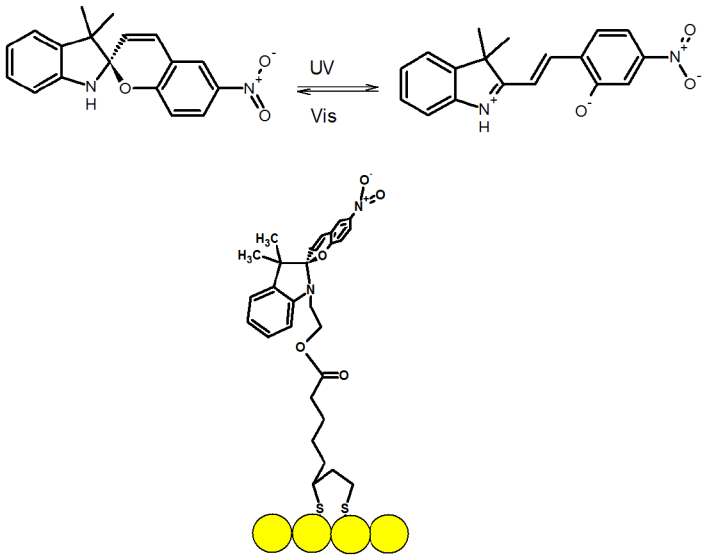

Figure 1. Interconversion between the closed SP– and the open MC–form under irradiation with light for a 6–Nitro–BIPS unit. Below 2–(3'3'–Dimethyl–6–nitro–3'*H*–spiro[chromene–2,2'–indol]–1'–yl)ethyl(1,2–dithiolane–3)pentanoate (SP-LA) attached on a gold surface as used in this study.

2. Experimental

2.1. Sample preparation

As described above, in this study we construct SAMS of 2-(3′,3′-dimethyl-6-nitro-3′H-spiro[chromene-2,2′-indol]-1′-yl)ethyl (1,2-dithiolane-3)-pentanoate (SP-LA). This molecule is synthesized following Tomasulo et al [28] in a one-step procedure using commercially available reagents. In summary, the generic spiropyran, *i.e.* 1-(2-hydroxyethyl)-3,3-dimethylindolino-6′-nitrobenzopyrylospiran (from TCI America) is treated with (±)-α-lipoic acid in the presence of N,N′- dicyclohexylcarbodiimide and 4-dimethylaminopyridine and the resulting ester isolated.

We investigated our optically switchable SAM in a thin film spectroelectrochemical cell that has been previously described [29]. In brief, thin films of gold with a thickness of 200 nm were deposited on a glass disc via chemical vapor deposition in the electrode arrangement shown in Figure 2. After deposition all gold surfaces were cleaned using a series of solvents: successively chloroform, ethanol and water. After solvent cleaning steps all electrodes were annealed with a propane gas/oxygen flame and exposed to UV/ozone (ProCleaner^{TM}, Bioforce Nanoscience) for 30 minutes. After all cleaning steps the SAM was formed on the working electrode (the circular portion delineated in Figure 2) by exposing it to a SP-LA dichlormethane (DCM) solution (0.5 mM) following previous procedures [22]. After 24 h the sample was rinsed with DCM and immediately used in the experiment. The gold electrodes were connected to a potentiostat (VSP, Bio–Logic

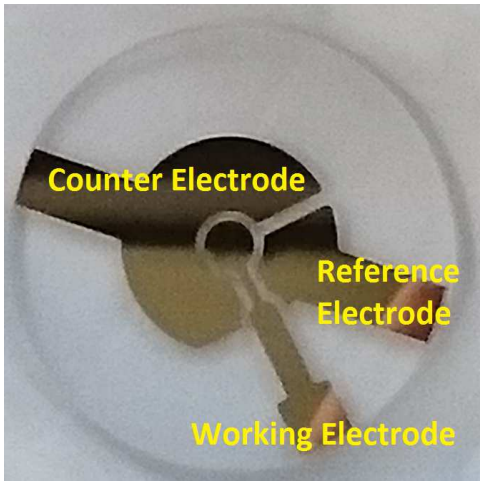

Figure 2. Thin film electrode as used during this study.

Science Instruments), the disc covered with a 50 μm teflon spacer and a CaF_2 window and the cell filled with a 0.1 M solution of Tetramethylammonium hexafluorophosphate (TMAH) in deuterated acetonitrile (Aldrich). The spacer is sized such that all three electrodes are covered by electrolyte. We verified that the Au pseudo-ref electrode was, in fact, a reference and calibrated it relative to a standard mercury sulfate reference

electrode (MSE) by comparing open circuit potentials and the dimerization peak (see discussion below) measured vs. an MSE reference electrode and the gold pseudo-ref.

The choice of appropriate solvent for this experiment requires balancing several competing demands. In brief, previous work has shown that for spiropyrans dissolved in solution an excessively polar solvent leads to an irreversible stabilization of the MC form: optical switching is no longer possible [17]. While this effect is less pronounced in SAMS, where the type of solid to which the spiropyran is attached appears to play a larger role [30, 17], we clearly wish to avoid such influence. To conduct this study, however, a solvent was also required that is sufficiently polar to allow easy dissolution of an electrolyte. Finally, as discussed in detail below, because in our sample geometry the incident infrared field must pass through the solvent, we also require a solvent that is only minimally absorptive in the IR from 1200-1700 cm^{-1}. After a series of preliminary experiments with different solvents we settled on deuterated acetonitrile as a the best compromise for these diverse requirements.

2.2. VSF-Spectroscopy

2.2.1. Experiment To conduct a VSF measurement we overlap spatially and temporally infrared and visible layers and measure the intensity of the emitted light at the sum of the frequencies of the two incident fields. The laser system we employ to create this spectrometer is described elsewhere in detail [31, 29]. In summary, the system contains a Ti:Saphire oscillator (Venteon, Femtoseconds Laser Technologies) and a regenerative amplifier (Legend Elite Duo HE+ and Cryo PA, Coherent). One half of the output of the regenerative amplifier (7.5 mJ/pulse, 45 fs pulses, 1 kHz, center frequency 800 nm) pumps a commercial optical parametric amplifier (HE-TOPAS, Light Conversion) yielding a signal and idler output mixed in a non-collinear Difference Frequency Generation scheme, to produce gaussian shaped broadband infrared (FWHM=300 cm^2) pulses, whose center frequency was tuned to 1390 cm^{-1}. The residual of the TOPAS was used to create a narrow band visible (VIS) pulse at 12,500 cm^{-1} (*i.e.* 800 nm) with a bandwith of 10 cm^{-1}. A band pass filter centered at 800 nm filtered out any higher order components from the TOPAS/DFG steps transmitted through the etalon.

The IR and VIS pulses hitting the sample surface were controlled each with a $\lambda/2$ plate, polarizer, $\lambda/2$ plate combination and were set to 10 μJ and 8 μJ per pulse respectively. The two beams were directed such that they are coplanar (and this plane perpendicular to the plane of the surface) and focused on the sample (see Figure 3) using lenses with focal lengths of 700 mm and incident angles of 40.4±0.5 and 65±0.5 for the IR and VIS were they were spatially and temporally overlapped. The VSF signal emitted from the sample was collimated, and dispersed afterwards in a spectrograph (ISA Triax Series 320, HORIBA Jobin Yvon GmbH) and detected on an emICCD Camera (PI–MAX® 4, Princeton Instruments). All spectra shown here were collected employing a *ppp* polarisation condition (both incident and the emitted field polarized parallel to the

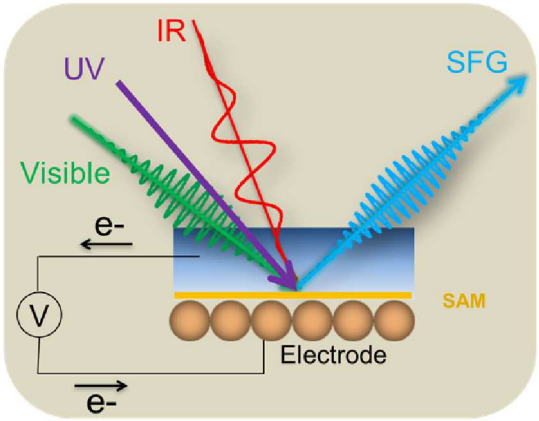

Figure 3. Schematic of our thin-film spectroelectrochemical cell. Two probing beams (IR and VIS) are overlapped together in time and space (to photoswitch with an additional UV beam) at a gold electrode, on which a bias can be applied, to yield an VSF–signal.

plane of incidence). To photoswitch the SAM from the SP to MC forms we continuously irradiated the sample with a UV laser (wavelength 355 nm, pulse duration 10 ns, repetition rate 10 kHz, CryLas). The pulse fluence was set to 0.1 μJ ($2.28*10^{13}$ photons mm^{-2} second^{-1}) using filters. All measurements were conducted while flushing the IR beam path with Nitrogen (to avoid absorption by water vapour at bend frequencies) and in other respects under ambient conditions. For all spectra the acquisition time was 1 min. The raw spectra we obtained were corrected for the, frequency dependent, IR energy by dividing all spectra by a reference signal from gold.

2.2.2. Data Analysis Much previous work has found that the variation in I_{VSF} as a function of the frequency of the incident IR field can be described as a coherent superposition of a nonresonant contribution and one or more resonances [26]:

$$I_{VSF} \propto ||\chi^{(2)}_{NR}|e^{i\Phi_{NR}} + \sum_j |\chi^{(2)}_{R,j}(\nu_{IR})|e^{i\Phi_j}|^2 I_{VIS} I_{IR}(\nu_{IR}) \quad (1)$$

where ν_{IR} is the frequency of the incident IR field, $\chi^{(2)}_{NR}$ the second order susceptibility of the non resonant and $\chi^{(2)}_{R,j}$ the frequency dependent second order susceptibility of the j^{th} resonance, Φ_{NR} the phase of the nonresonant, and Φ_j the phase of the j^{th} resonance. If these resonances are homogenously broadened, and the effect of dynamics or mode coupling on the line shape small, each resonance can be described as a Lorentzian,

$$\sum_j |\chi^{(2)}_{R,j}(\nu_{IR})|e^{i\Phi_j} \propto \sum_j \frac{A_j e^{i\Phi_{j'}}}{\nu_j - \nu_{IR} - i\Gamma_j} \quad (2)$$

with A_j the amplitude, ν_j the resonance center frequency and Γ_j the damping constant of the j^{th} vibration. The emitted VSF field is interface specific by its symmetry selection rules. These symmetry restrictions manifest on the molecular level by the requirement

that only modes that are both infrared and Raman active are visible in the resonant VSF response.

As discussed above all VSF measurements were conducted under the *ppp* polarization condition. Given coplanar, copropagating incident beams (plane of incidence normal to the surface) and a surface with macroscopic $C_{\infty\nu}$ symmetry, $\left|\chi_R^{(2)}\right|^2$, for all modes we characterize, is proportional to the amplitude of the component of the IR transition dipole along the surface normal (see Supporting Information for detailed discussion of this point and prior reviews [26]).

3. Results and Discussion

As discussed above, we are interested in understanding the switching behavior of our 6–Nitro–BIPS SAM as a function of applied electric field but in the absence of charge transfer or interfacial chemistry. To determine the potential range in which such a condition can be achieved we collected cyclic voltammograms in our spectroelectrochemical cell. Representative results are shown in Figure 4.

In the first cycle an irreversible oxidation takes place at +0.56 V with respect to a standard mercury sulfate electrode(MSE). This oxidation has been observed previously for a 6–Nitro–BIPS SAM [32] and assigned to the formation of dimers in the SAM. As the second (and all subsequent) scan illustrates, dimer formation is irreversible. This dimerization, and the subsequent oxidation, requires transfer of 2 electrons and thus the oxidation peak current density furnishes a lower bound of SP-LA density. In our hands we found the surface density of SP-LA in our SAM to be $(3.4\pm1)*10^{-11}\frac{mol}{cm^2}$ or one molecule per 4.8 nm^2. Because the diameter of the 6–Nitro–BIPS headgroup is $\approx$ 1 nm and the spacer by which it is attached to the electrode is also $\approx$ 1 nm long we expect that individual chromophores may interact sterically. At sufficiently cathodic potentials, below -1.2 V, we observe a significant current that is *reversible* (see Supporting Information for data). Prior studies have observed an irreversible feature at these potentials and assigned it to the reduction of NO_2 [33]. Conducting a CV without the SAM (see Supporting Information for data) suggests that this reduction peak we observe here is a characteristic of the electrolyte and that this current is sufficiently large to obscure the reduction of NO_2 in the first cycle. Continuing to still more cathodic potentials it is also possible to drive reduction of the S in the anchoring thiolate group and cause irreversible desorption of the adsorbed SAM [24]. To investigate field effects on our spiropyran SAM we require a potential range that avoids all such electron transfer processes. Taken together the data in Figure 4 and the additional CVs shown in the Supporting Information suggest that, starting with a pristine, non-oxidized SAM, and restricting ourself to potentials from $-0.8 - +0.2$ vs. MSE, any changes in photostationary state or structure of the SAM will be the result of the interfacial field.

Given this attachment density, and window of potential stability of our SAM, the first step in understanding the effect of interfacial field on SP/MC relative stability is understanding the spectral response of each form at the Au electrode in contact with

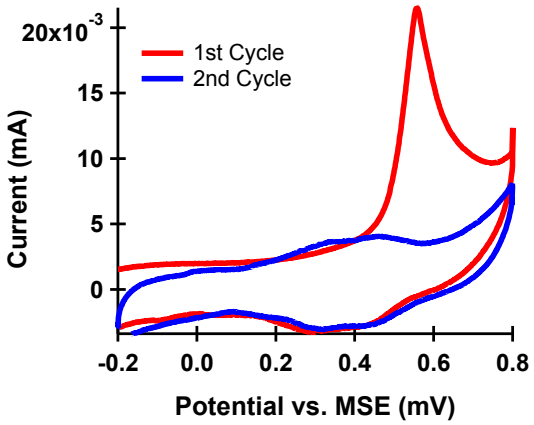

Figure 4. Cyclic Voltammogram of our SP-LA SAM on a gold electrode vs an MSE reference at a 50 mV/sec scan rate. In the first run at +0.56 V an irreversible oxidation takes place leading to a new species at the surface that shows reversible redox behavior in the second and all further scans.

acetonitrile. A VSF spectrum of SP-LA attached to a gold electrode, under open circuit potentials, in contact with deuterated acetonitrile is shown both in its closed, Spiropyran (SP), form and, after irradiation with UV light, in its presumably open, Merocyanine (MC) form in Figure 5. Encouragingly there is a significant spectral change on irradiation. To relate these changes to structural change a quantitative line shape analysis is required. As discussed above VSF activity requires a mode to be both Raman and infrared active. Prior studies make clear that there are eight modes, with frequencies 1250-1650 cm^{-1}, that are both IR and Raman active for 6–Nitro-BIPS [34, 35].

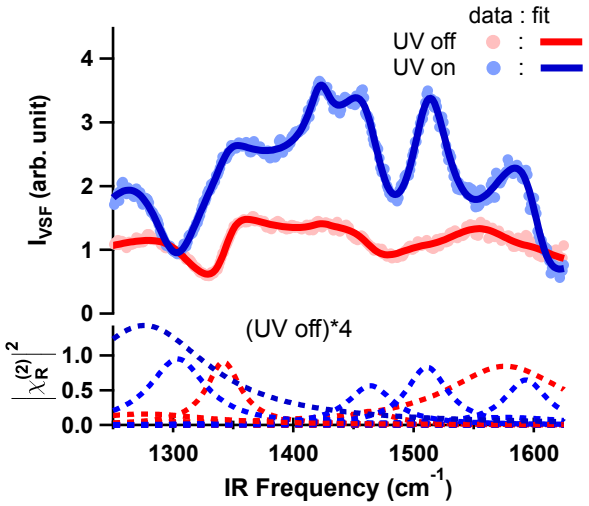

Figure 5. Measured and fitted VSF-Spectrum at open current potential without (red) and with UV irradiation(blue).

Reference to Figure 5 and Table 1 makes clear that the dominant feature in the

Table 1. Observed vibrations in the VSF-spectra of SP–LA in its open SP– and its closed MC–form and their assignments compared to reference values.[34, 35]

Resonance Freq (cm^{-1})			**Assignment**
UV off	UV on	Reference	
1276	1276	1278	C–N
1304	1304	1307	$C–N^+$
1342	1342	1336	NO_2^{sym}
—	1423	1426	$C–O^-$
1464	1464	1460	CH_3^{asym}
—	1511	1509	NO_2^{asym}
1576	1576	1570	δ aromatic
—	1593	1593	$C{=}N^+$

spectrum of the closed SP–form is the NO_2^{sym}–stretch (*i.e* the NO_2 symmetric stretch) located at 1339 cm^{-1}. Minor features at 1273, 1466, and 1565 cm^{-1} can be assigned to the C-N stretch, the CH_3^{asym} bend and aromatic deformation respectively. Strikingly, a small feature also appears at 1312 cm^{-1} in the absence of UV irradiation that can be assigned to the $C–N^+$ stretch. If our assignment is correct the presence of this resonance in the absence of UV irradiation suggests that our monolayer contains small amount of the open, MC form, in the absence of irradiation and that this resonance intensity should increase dramatically when the UV light is turned on. In agreement with this expectation, after UV irradiation the 1312 cm^{-1}, $C–N^+$ feature increases dramatically in amplitude and the complementary $C–O^-$ stretch at 1423 $^{-1}$ is now apparent. Clearly the $C–N^+$ intensity is much larger than than the $C–O^-$. As discussed above, this ratio is most simply explained if the $C–O^-$ transition dipole is nearly parallel to the Au surface while the $C–N^+$ is perpendicular (see detailed discussion and sensitivity tests of this effect in the Supporting Information).

While the $C–N^+$ and $C–O^-$ modes are characteristic of the open MC form, clearly probing modes that exist in both the SP and MC forms, *e.g.* the NO_2 symmetric and asymmetric stretch, offer the potential for insight into conformational change of the 6–Nitro-BIPS on switching. Because the transition dipoles of the NO_2^{sym} and NO_2^{asym} stretches must be orthogonal, and because, as discussed above, absolute intensities increase for transition dipoles oriented closer to the surface normal, comparison of the relative intensities of these modes after and before irradiation should offer insight into the change in orientation of the NO_2 moiety on irradiation. Inspection of the data and fits in Figure 5 makes clear that in the absence of irradiation the NO_2^{sym} response is dominant while after irradiation the NO_2^{asym} response is now large.

While the relative $\left|\chi_R^{(2)}\right|^2$ of different modes offers some constraints on SAM structure, additional structural insight can be obtained from data of the type shown in Figure 5. As is shown in equation 1 (and reviewed in detail in the Supporting Information) the measurement of I_{VSF} at any frequency reflects the interference between the non-resonant

portion of the signal and one (or more resonances). If this interference is constructive, and $|\chi^{(2)}_{\mathrm{NR}}| \geq |\chi^{(2)}_{\mathrm{R}}|$, the resulting spectral response will appear as a peak on top of the broad non-resonant feature, if destructive it will appear as a dip. Given a known, UV independent nonresonant phase of Au (measured to be $\pi/2$ by previous workers [26, 36]) all changes in phase must reflect changes in Φ_j. As has been discussed in detail in prior work, and is derived in the Supporting Information for our SAM system and modes of the symmetry that we consider, *peaks* suggest a transition dipole pointed towards the Au surface, *dips* one pointed away.

Given this logic returning to the NO_2^{sym} stretch (at 1334 cm^{-1}) offers additional insight: clearly in the absence of UV irradiation the NO_2^{sym} feature at 1334 cm^{-1} appears as a strong dip (indicating its transition dipole points nearly along the surface normal and away from the Au) while under irradiation it appears as a very weak peak (suggesting its transition dipole is now nearly parallel to the surface but pointing slightly toward the Au). Conversely, the 1513 cm^{-1} peak of the NO_2^{asym} is absent in the SP form and appears as a clear peak in the open MC form suggesting that under UV irradition *its* transition dipole points towards the Au surface and is nearly perpendicular. Similarly the C-N^+ resonance appears as a strong dip in after UV irradiation, suggesting that its transition dipole points, as expected, away from the Au surface and is nearly perpendicular. Finally the C-N^+ complementary stretch, the C-O^+, also appears as a weak dip in the MC spectra: under UV irradiation the transition dipole of the C-O^+ points towards the Au but is nearly parallel to the plane of the surface. These considerations suggest the structure changes between the SP and MC form as shown in Figure 6 on photoswitching.

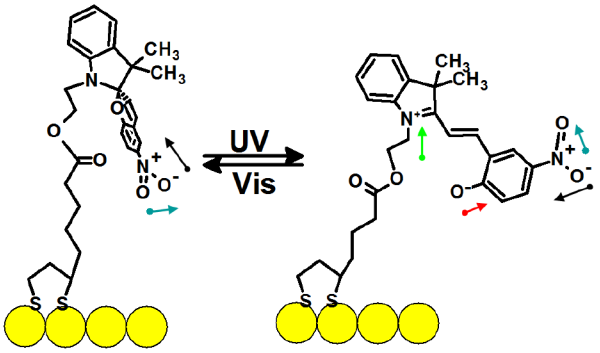

Figure 6. Change of dipole moment direction during switching, giving rise to changes in the 6-Nitro-BIPS-spectrum. The dipole moments of NO_2^{sym}(black), NO_2^{asym}(blue), C–N^+(green) and C–O^-(red) are shown.

Because both the SP and MC forms of 6-Nitro-BIPS are polar, one might expect that it is possible to induce changes in chromophore orientation, in either form, in our SAM (or more broadly in any surface immobilized spiropyran) without irradiation by addition of solvent [37, 17]. In particular, by adding a *polar* solvent we might expect to induce structure change in the SAM. We tested this expectation by collecting VSF spectra of the SP-LA monolayer in air and in acetonitrile in the absence of UV irradiation

(see Figure 7). While collected only over a restricted frequency range in the IR these spectra clearly show that the NO_2^{sym} appears as a peak in air and a dip in acetonitrile: the transition dipole of the NO_2^{sym} points towards the Au surface in air and away in contact with acetonitrile.

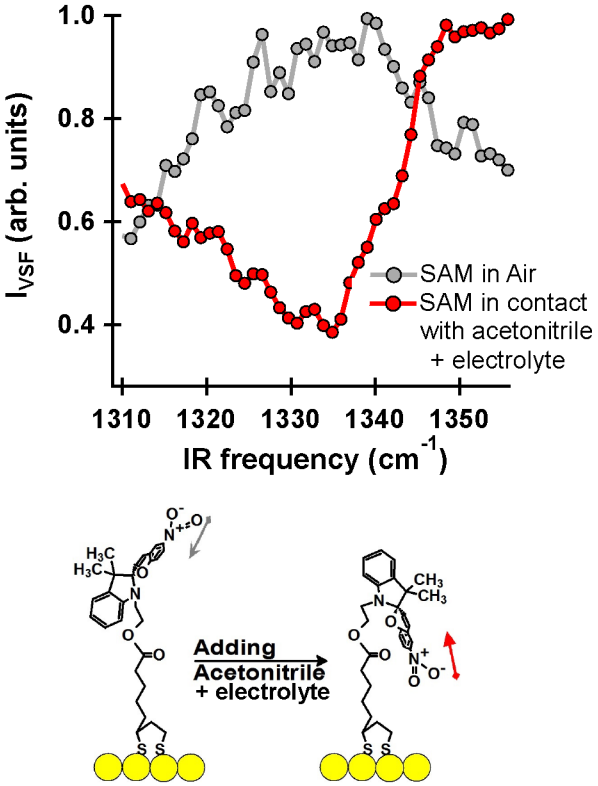

Figure 7. Spectra of the symmetric NO_2–stretch in the SAM containing gold electrode in air (grey) and with added Tetrabutylammonium hexafluorophosphate containing Acetonitrile as electrolyte (red). Below molecular rearrangement and change of the dipole moments orientation that causes spectral change.

Given insight into the switching of our spiropyran SAM in contact with acetonitrile at open circuit potentials, and constraints on how adding acetonitrile changes the 6–Nitro-BIPS orientation relative to the same SAM in air, we next examined the effect of changing interfacial potentials. Much prior work has shown that spiropyrans can switch under a wide range of external stimuli [38, 39, 40, 17]. Accordingly we first determined whether our SP-LA can be switched from its SP to its MC-form solely by applying a bias. Inspection of the results in Figure 8 shows that this is clearly not possible: the spectral response at all potentials investigated is quantitatively similar to that measured under open circuit potentials (*n.b.* the open circuit potential in our spectroelectrochemical cell in the absence of UV irradiation is -0.21 V vs. MSE) for the SP form in Figure 5 and bias independent. Quantitative line shape analysis (see Supporting Information for details) suggests that this can be well described with potential independent center frequencies for all modes: there is no observed Stark shift. The absence of a Stark shift

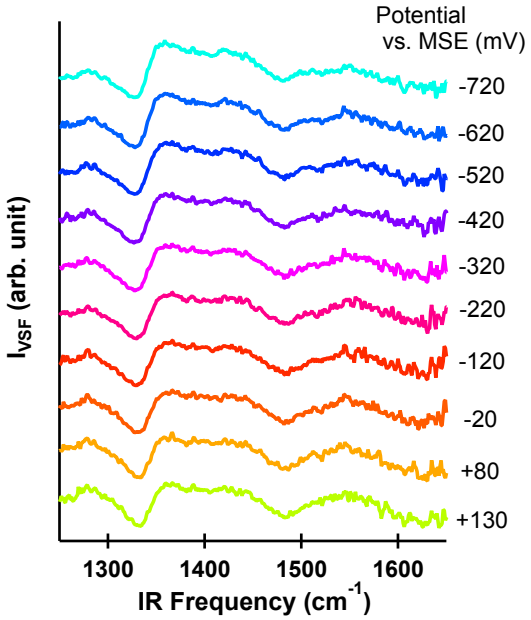

Figure 8. Potential dependent measurements of the SP–LA SAM without additional irradiation. I_{VSF} spectra are offset for clarity. There are small, potential dependent, differences in the nonresonant portion of I_{VSF} (see Supporting Information for details).

for the SP-LA form is consistent with prior work by Berkovic et al. studying similar chromophores dissolved in solution in which only the MC-form was found to exhibit a Stark shift (where the difference is presumably the result of the larger π-electronic system in the MC form) [41]. We have discussed at some length above (and in the Supporting Information) how the measured I_{VSF} spectral response depends on molecular orientation. It is worth noting that one additional implication of the data shown in Figure 8 is that the SP-LA monolayer structure is *not* potential dependent. Evidently the dipole of the SP chromophore is sufficiently small (presumably near the 5D known from solution), and the packing density of the SAM sufficiently large, that its orientation does not change in applied fields of the amplitude we employed.

Since the electric field did not induce a switch we went back to -220 mV and irradiated the sample with UV-light obtaining a photostationary spectrum quantitatively similar to that shown in Figure 5. We then altered bias while continuously irradiating with UV (see Figure 9). One way of understanding this experiment is that we probed the stability of the MC form, in the UV induced photostationary state, as a function of applied bias. Inspection of the data in Figure 9 clearly shows that changing potential from positive to negative leads to the increasing *destabilization* of the MC form relative to the SP, in the photostationary state.

As noted above, in the potential window explored in this data we expect the only effect of surface potential is to introduce an interfacial static electric field. As the dipole moment of the 6-Nitro-BIPS chromophore in its open, MC form is large relative to

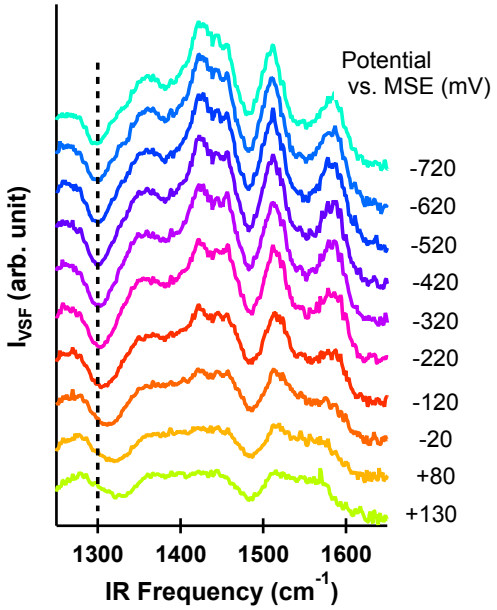

Figure 9. Potential dependent measurements under continuous irradiation with UV light.

it in the SP (16 D vs. 5 D) and the structure, and attachment density, of molecules in the SAM may restrict the orientation of the chromophore in this field, the relative destabilization of the MC is most simply rationalized as a consequence of its large dipole moment's inability to assume an energetically favorable orientation in the interfacial field due to steric constraints.

Inspection of the the data in Figure 9 clearly illustrates the relative destabilization of the MC form with increasingly negative potentials. However it is difficult to understand, without further analysis, whether the structure of the MC dominated monolayer, *i.e.* at potentials more negative than $\approx$ 420 mV in Figure 9, is potential dependent. To explore this scenario we fit the data with the line shape model described above, extracted the amplitudes of the NO_2^{asym} and C-N^+ modes (see Figure 10, all amplitudes are normalized by their value at the potential at which they are largest). The C-N^+ mode occurs only in the MC form and thus its increasing amplitude must, at least in part, reflect an increasing [MC]:[SP] ratio. While the NO_2^{asym} is present in both states, as the data at open circuit potentials in Figure 5 show, it's clear that the structure of the SAM is such that it is large in MC dominated samples. Both amplitudes reveal a similar trend: as one shifts towards more negative potentials the [MC]:([SP]+[MC]) ratio in the irradiated monolayer increases from 0 towards 1.

Interestingly, however, while the C-N^+ stretch reaches a maximum amplitude at -420 mV it then decreases, by $\approx$ 20%, with increasingly negative potentials while the NO_2^{asym} monotonically increases. Because the C-N^+ is specific to the MC form, and because its position on the alkyl chain suggests its orientation should be less sensitive to an applied

field than the NO_2 group on 6–Nitro-BIPS, the simplest explanation for this discrepancy is that with potentials negative of -420 mV the 6–Nitro–BIPS chromophore reorients in such a way that the NO_2^{asym} amplitude continues to increase, while the [MC]:([SP]+[MC]) ratio is decreasing. The observation that the structure of the MC dominated SAM is, apparently, potential dependent, while that of the SP dominated SAM is not (as shown in Figure 8) is consistent with the much larger dipole of the MC.

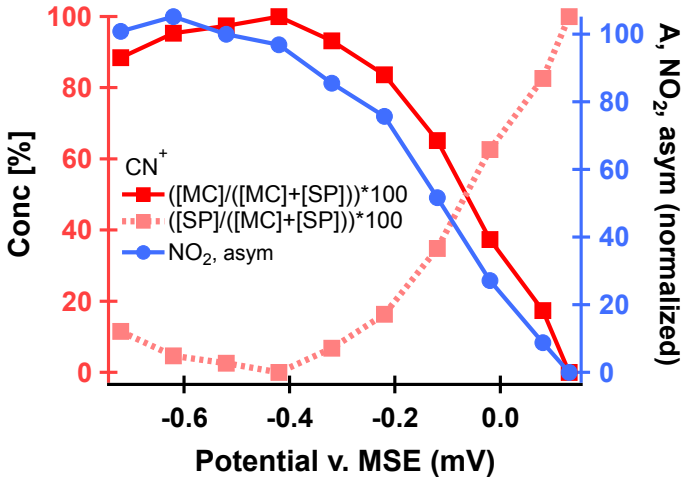

Figure 10. Amplitudes' change as a function of applied potential for the C–N^+– and C–O^-–stretch that are unique to the MC–form.

The change in structure and [MC]:([SP]+[MC]) ratio of our UV irradiated SAM has both benefits and drawbacks for the use of 6–Nitro–BIPS on monolayer electrodes for sensing. On the benefit side of the ledger the applied potential allows one to switch between the *on* and *off*-state of the electrode both faster and more completely than thermal stimuli (and at least for this SAM in air using VIS irradiation [22]). In particular by cycling our electrode to positive potentials, on $\approx$ 1 minute time scales, we recover a SAM with essentially no [MC] form. As noted above, at open circuit potentials, removing UV irradiation causes a relaxation back to an [SP] dominated monolayer on timescales of hours with a [MC]:([SP]+[MC]) that is nonzero. Prior work by some of us has shown that it is possible to optically switch this SAM in contact with air from the [MC] to [SP] forms using visible light irradiation on a timescale of ten minutes [22]. We did not test this possibility for the SAM in contact with acetonitrile but clearly the ability to switch this monolayer via potential perturbation removes complexity from any sensor (*e.g.* light at only one wavelength is requried). On the drawback side, the potential dependent structure and composition of the UV irradiated photostationary state limits the potential range under which one can electrochemically detect any desired species: the potential range in which the sensor can be switched *on*/*off* is given by the potential range over which the bistable SAM can be optically switched.

4. Summary and Conclusions

Creation of electrochemical sensors using photo-switchable self-assembled monolayers as gates or sensitizers, requires quantitative understanding of how the interfacial field effects the properties of the photoswitch. In this study we show, employing interface-specific vibrationally resonant sum frequency spectroscopy, that for a self-assembled monolayer of SP-LA on an Au electrode moderate interfacial fields have pronounced effects on the switching behavior. In particular, under continuous UV irradiation the application of negative bias leads to a photostationary state dominated by the open MC form which while a positive bias favors formation of the closed SP. Because this effect is large, a change in interfacial potential of 0.2 V can alter the ratio of the MC and SP forms by a factor of 2, rapid interconversion between the SP and MC forms of the SAM can be achieved by potential cycling. Results of this type are important for the application of SP-LA in the sensing schemes described above, they define the potential range over which this sensor could be switched *on* and, inversely, the potential range at which it can be switched *off* when excess analyte needs to be removed. We expect that the effects of interfacial field we observe on the 6–Nitro-BIPS containing SAM to be general. Any SAM containing a bistable, optically switchable chromophore whose two states differ significantly in dipole moment should show similar, field induced effects on photostationary state composition and structure. Accounting for these effects is clearly critical in the application of any of these constructs in quantitative sensing.

5. Acknowledgements

The authors thank the Deutsche Forschungsgemeinschaft for support of this study through Collaborative Research Center 658: Elementary Processes in Molecular Switches at Surfaces.

6. References

[1] Vlassiouk I, Park C D, Vail S A, Gust D and Smirnov S 2006 *Nano Letters* **6** 1013–1017
[2] Areephong J, Browne W R, Katsonis N and Feringa B L 2006 *Chemical Communications* 3930–3932
[3] Katsonis N, Lubomska M, Pollard M, Feringa B and Rudolf P 2007 *Progress in Surface Science* **82** 407–434
[4] Crivillers N, Orgiu E, Reinders F, Mayor M and Samorì P 2011 *Advanced Materials* **23** 1447–1452
[5] Marchante E, Crivillers N, Buhl M, Veciana J and Mas-Torrent M 2016 *Angewandte Chemie International Edition* **55** 368–372
[6] Willner I, Blonder R and Dagan A 1994 *Journal of the American Chemical Society* **116** 9365–9366
[7] Blonder R, Willner I and Bckmann A F 1998 *Journal of the American Chemical Society* **120** 9335–9341
[8] Wang G, Bohaty A K, Zharov I and White H S 2006 *Journal of the American Chemical Society* **128** 13553–13558
[9] Xie X, Mistlberger G and Bakker E 2012 *Journal of the American Chemical Society* **134** 16929–16932
[10] Tao J, Li Y, Zhao P, Li J, Duan Y, Zhao W and Yang R 2014 *Biosensors and Bioelectronics* **62** 151–157

[11] Tao J, Zhao P, Li Y, Zhao W, Xiao Y and Yang R 2016 *Analytica Chimica Acta* **918** 97–102
[12] Anzai J I, Sakamura K, Hasebe Y and Osa T 1993 *Analytica Chimica Acta* **281** 543–548
[13] Bléger D and Hecht S 2015 *Angewandte Chemie International Edition* **54** 11338–11349
[14] Bléger D 2016 *Macromolecular Chemistry and Physics* **217** 189–198
[15] Lahann J, Mitragotri S, Tran T N, Kaido H, Sundaram J, Choi I S, Hoffer S, Somorjai G A and Langer R 2003 *Science* **299** 371–374
[16] Görner H 2001 *Physical Chemistry Chemical Physics* **3** 416–423
[17] Klajn R 2014 *Chemical Society Reviews* **43** 148–184
[18] Alemani M, Peters M V, Hecht S, Rieder K H, Moresco F and Grill L 2006 *Journal of the American Chemical Society* **128** 14446–14447
[19] Henzl J, Bredow T and Morgenstern K 2007 *Chemical Physics Letters* **435** 278–282
[20] Wolf M and Tegeder P 2009 *Surface Science* **603** 1506–1517
[21] Piantek M, Schulze G, Koch M, Franke K J, Leyssner F, Krger A, Navo C, Miguel J, Bernien M, Wolf M, Kuch W, Tegeder P and Pascual J I 2009 *Journal of the American Chemical Society* **131** 12729–12735
[22] Darwish T A, Tong Y, James M, Hanley T L, Peng Q and Ye S 2012 *Langmuir* **28** 13852–13860
[23] Ivashenko O, van Herpt J T, Feringa B L, Rudolf P and Browne W R 2013 *Langmuir* **29** 4290–4297
[24] Love J C, Estroff L A, Kriebel J K, Nuzzo R G and Whitesides G M 2005 *Chemical Reviews* **105** 1103–1170
[25] Nuzzo R G and Allara D L 1983 *Journal of the American Chemical Society* **105** 4481–4483
[26] Lambert A G, Davies P B and Neivandt D J 2005 *Applied Spectroscopy Reviews* **40** 103–145
[27] Vidal F and Tadjeddine A 2005 *Reports on Progress in Physics* **68** 1095–1127
[28] Tomasulo M and Ibrahim Yildiz F M R 2007 *Inorganic Chimica Acta* **360** 938–944
[29] Tong Y, Cai K, Wolf M and Campen R K 2016 *Catalysis Today* **260** 66–71
[30] Klajn R, Stoddart J F and Grzybowski B A 2010 *Chemical Society Reviews* **39** 2203
[31] Tong Y, Wirth J, Kirsch H, Wolf M, Saalfrank P and Campen R K 2015 *The Journal of Chemical Physics* **142** 054704
[32] Ivashenko O, van Herpt J T, Feringa B L, Rudolf P and Browne W R 2013 *The Journal of Physical Chemistry C* **117** 18567–18577
[33] Katz E, Lion-Dagan M and Willner I 1995 *Journal of Electroanalytical Chemistry* **382** 25–31
[34] Florea L, Hennart A, Diamond D and Benito-Lopez F 2012 *Sensors and Actuators B: Chemical* **175** 92–99
[35] Delgado-Macuil R, Rojas-Lpez M, Gayou V, Ordua-Daz A and Daz-Reyes J 2007 *Materials Characterization* **58** 771–775
[36] Potterton E A and Bain C D 1996 *Journal of Electroanalytical Chemistry* **409** 109–114
[37] Dübner M, Spencer N D and Padeste C 2014 *Langmuir* **30** 14971–14981
[38] Darwish T A, Evans R A, James M, Malic N, Triani G and Hanley T L 2010 *Journal of the American Chemical Society* **132** 10748–10755
[39] Darwish T A, Evans R A, James M and Hanley T L 2011 *Chemistry: A European Journal* **17** 11399–11404
[40] Darwish T A, Evans R A and Hanley T L 2012 *Dyes and Pigments* **92** 817–824
[41] Berkovic G, Krongauz V and Weiss V 2000 *Chemical Reviews* **100** 1741–1754